CrossMark

# Analysing the Combined Effect of Barrier Wall and Freshwater Injection Countermeasures on Controlling Saltwater Intrusion in Unconfined Coastal Aquifer Systems

Asaad M. Armanuos[1] · Mona G. Ibrahim[2] · Wael Elham Mahmod[2,3] · Jiro Takemura[4] · C. Yoshimura[5]

## Abstract

Freshwater recharge wells and underground flow barriers are among several methods proposed for controlling saltwater intrusion (SWI) into coastal aquifers. In this study, experimental and numerical studies were performed to determine the effect of using a flow barrier wall, a recharge well and a combination of these, to control SWI in unconfined coastal aquifer systems. The SEAWAT model was used to predict the SWI wedge and the behaviour of the retreating residual saltwater after installing the remediation measures. The results show that increasing the barrier wall embedment ratio ($d_b/d$) from 0.44 to 0.67 led to an increase in the repulsion ratio (R) from 20.8 to 46.87%. Moreover, increasing the freshwater injection rate ratio ($Q_i/Q$) from 0.22 to 0.56 increased the repulsion ratio (R) from 10.93 to 22.39%. Barrier wall embedment with ratios ($d_b/d$) of 0.44, 0.51 and 0.57, combined with a freshwater injection ratio ($Q_i/Q$) with a value of 0.56, achieved (R) of 41.14, 45.41 and 50.0%, compared with 20.8, 27.1 and 34.40% for the barrier wall only and 22.39% for freshwater injection only. Freshwater injection ratios ($Q_i/Q$) of 0.22, 0.33, 0.44 and 0.56 combined with a barrier wall embedment ratio ($d_b/d$) of 0.508 achieved repulsion ratios (R) of 33.9, 36.5, 39.0 and 45.42%, compared with 10.9, 15.6, 18.8 and 22.4% respectively for freshwater injection only and 27.1% for the barrier wall only. A combination of flow barrier and freshwater injection forced the saltwater to retreat and achieved values of R greater than either the barrier wall or freshwater injection separately.

Keywords Saltwater intrusion · Freshwater injection · Barrier wall · Combination

✉ Asaad M. Armanuos
asaad.matter@f-eng.tanta.edu.eg

Extended author information available on the last page of the article

🖄 Springer

# 1 Introduction

Groundwater in coastal aquifers is a major source of freshwater supplies in many areas all over the world. Groundwater abstraction in coastal aquifers leads to depletion of groundwater levels and decreases the freshwater flow towards the sea. Consequently, saltwater intrusion (SWI) into inland (coastal) aquifers leads to deterioration in the quality of the groundwater and threatens this important fresh groundwater supply (Luyun 2010). Climate system warnings led to change in the variable of the climate and extreme climate conditions (Luo et al. 2018a, b). The rise in the sea level as a result of climate change will accelerate the degree of SWI. According to the Intergovernmental Panel on Climate Change (IPCC), the sea level will rise by 0.52 to 0.98 m by the year 2100, (IPCC 2013). Anwar (1983) investigated the effect of using cut-off walls on the control of SWI. Based on the sharp interface approach, an analytical relationship was developed to determine the location of the saltwater interface in the case of a single cut-off wall.

Hasan Basri (2001) applied implicit and explicit simulation-optimization approaches to develop two new methods to increase the cost-effectiveness of using a subsurface cut-off wall to control SWI. Anwar (1983), Luyun et al. (2009, 2011), Abdoulhalik et al. (2017) and Abdoulhalik and Ahmed (2017) performed laboratory experiments to explore the effect of using underground barriers as a control method for SWI. Luyun et al. (2011) investigated the effectiveness of flow barrier walls on controlling SWI in unconfined coastal aquifers, based on laboratory experiments using different depths and distances from the coast. In addition, Luyun et al. (2011) performed separate laboratory experiments to model the effect of freshwater injection through a well. The results showed that injecting the recharge water near to the toe of the seawater wedge led to an increase in the seawater repulsion ratio. Abdoulhalik et al. (2017) developed a new mixed physical barrier combining a barrier wall and a semi-permeable dam. The new barrier supported the movement of saline water towards the sea and achieved considerable repulsion of the saltwater length. Abdoulhalik and Ahmed (2017) performed numerical and laboratory experiments to control SWI in stratified heterogeneous coastal aquifers. Bear (1979) described the technique of injecting freshwater through wells to control SWI. Bruington and Seares (1965) described the effect of a recharge-well facility for controlling SWI in Los Angeles County, California. The United States Environmental Protection Agency (USEPA) categorized SWI recharge wells as class V underground injection control (UIC) wells. More than 1185 recharge wells were reported to be in use in the USA (USEPA 2017). Hunt (1985) derived a steady-state solution for the freshwater-saltwater interface location for either single or multiple recharge wells, injecting freshwater into both confined and unconfined aquifers. Hunt's (1985) solution was based on the sharp interface approach, which was also used by Strack (1976) to derive solutions for abstraction wells. Hunt's (1985) solution is only applicable to freshwater injection through wells located on the landward interface side and not for those located at the SWI toe or within the SWI wedge itself. Luyun et al. (2009) studied experimentally and numerically the effect of using subsurface dams to prevent SWI and recover previously saline-intruded coastal aquifers for freshwater storage and supply. In this study, a sand box model was built to perform experiments to model the effect of using a barrier wall, a recharge well and a combination of both, to control SWI in unconfined coastal aquifers. The SEAWAT model was used to simulate the SWI experiments numerically. Finally, a comparative analysis was undertaken to compare the output repulsion ratio of the SWI for the barrier wall, the recharge well and the combination of both.

## 2 Experimental Settings

### 2.1 Sand Box Model

According to the experimental details shown in Fig. 1, the work was conducted in a sand box tank with length 74.4 cm, height 35 cm and width 10 cm. The freshwater reservoir is on the left side with a width of 10 cm, while the saltwater reservoir is on the right side with a width of 11 cm. Silica sand number 4.0 was used as the aquifer medium to model the unconfined coastal aquifer in the middle part of the sand box model. The sand was packed in layers with a thickness of 5.0 cm at each side of the sand box model, where the freshwater and the saltwater reservoirs were located. Specific gravity of soil sand grains $G_s = 2.64$, bulk density (saturated density) $=1.93$ g/cm$^3$ and dry density $= 1.50$ g/cm$^3$. Two pumps were used to feed the freshwater and the saltwater tanks through freshwater and saltwater feed pipes respectively. The freshwater and saltwater heads were controlled using an adjustable drainage pipe. Drainage pipe outflows were used to estimate the hydraulic conductivity and freshwater flow from the freshwater side to the saltwater side. Freshwater and saltwater pumps supplied water from two large constant-head tanks below the sand tank to the respective reservoirs with constant flow rates. A guide was fixed in the upper part of the sand tank for installing the barrier wall. The barrier wall was embedded in the sand box model at distance of 15.0 cm from the saltwater reservoir. Between the saltwater reservoir and the middle flow tank, a slot was used to insert the shut-off wall in order to separate the saltwater solution in the saltwater tank from the freshwater-filled porous medium tank, at the beginning of each experiment. Fine mesh screens and perforated acrylic sheets were used to separate the main tanks from the reservoirs on both sides. During sand packing, clamps were used to prevent extension and ensure a fixed width of the sand tank. The saltwater was prepared by dissolving salt in distilled water through several 10-L barrels to a concentration of 35,000 mg/L (sodium chloride). In order to distinguish the saltwater from the freshwater, the saltwater in the saltwater tank was dyed with a red food colouring at a concentration of 5 g dye per 10 L. A SALTMATE 100 device was used to measure the concentration of the saltwater. The density of the saltwater solution was 1025 kg/m$^3$, while the measured density of the freshwater was 1000 kg/m$^3$, as shown in Figure 1-A. For the flow barrier wall experiments, the wall was installed in the porous medium at distance of 15.0 cm from the saltwater reservoir and its depth was measured from the top level of the saltwater in the saltwater reservoir. Installing the flow barrier wall in the aquifer medium left an opening below the wall for the freshwater flow towards the saltwater reservoir in the bottom part of the aquifer medium. For the freshwater injection experiments, an additional pump was used for freshwater injection through a perforated pipe with a diameter of 1.0 cm and a length of 10.0 cm, with small pore holes in all directions. The perforated pipe was located at distance of 25.0 cm from the freshwater reservoir and at a depth of 10.0 cm from the bottom of the sand box model, as shown in Fig. 1.

### 2.2 Experimental Procedure

For the barrier wall and freshwater injection experiments, the porous medium tank and both side reservoirs were initially filled with distilled water. Drainage pipes were used to adjust the constant head to 31.4 and 30.5 cm, measured from the bottom of the sand tank reservoir for the freshwater and the saltwater reservoirs respectively. The estimated fluctuations of the head during the experiments were $\pm 1.0$ mm. The head difference between the freshwater and the
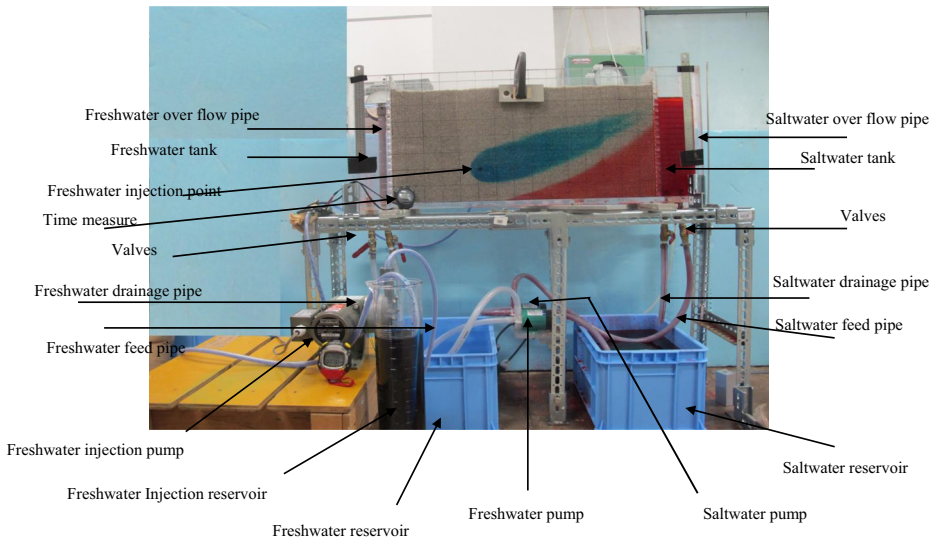
**Fig. 1** Sand box model

saltwater was 0.90 cm with hydraulic gradient (0.01209) is consistent with previous labora-
tories studies using similar experimental set up (Goswami and Clement 2007; Chang and
Clement 2012; Abdoulhalik et al. 2017) and within the range of hydraulic gradient measured at
some field sites (Attanayake and Sholley 2007). The hydraulic gradient between the two heads
produced a flow from the freshwater reservoir towards the saltwater reservoir. Darcy's law was
used to estimate the hydraulic conductivity (K) of the porous medium in the sand tank, based
on the hydraulic gradient and the measured freshwater flow from the drainage pipes. After
measuring the flow, the shut-off wall is then inserted to separate the saltwater reservoir from
the main middle tank. After that, the freshwater in the saltwater reservoir was removed and
replaced by the red saltwater solution from the saltwater tank below. The SWI process in the
aquifer medium was started by removing the shut-off wall between the saltwater reservoir and
the aquifer medium in the middle. At the beginning of each experiment, the freshwater head
and the saltwater head were both adjusted to 30.50 cm. The saltwater intruded inland into the
aquifer. The length of the SWI wedge reached 64.0 cm after 55.0 min (min.). After this time
the freshwater head was increased from 30.5 to 31.40 cm, whereas the saltwater head was
fixed throughout the experiment at 30.50 cm. After increasing the freshwater head, the head
difference between the freshwater and the saltwater reached 0.90 cm and the freshwater flow
forced the saltwater to retreat back towards the saltwater reservoir. The saltwater wedge
retreated gradually, and after 1 h (h) and 35 min. The SWI reached a steady-state condition
with length 48.0 cm, where no change in the toe position was observed. After reaching the
steady-state condition, various experiments on controlling the SWI using a barrier wall and
freshwater injection were performed. The length of the intruding saltwater wedge was
measured throughout the experiments. Photos were taken at various intervals, using a high-
resolution digital camera, for cross-checking with the recorded data. In the saltwater boundary
at the freshwater discharge zone, the freshwater flows vertically and floats over the saltwater in
the saltwater reservoir before draining out. Table 1-A summarizes the experimental procedures
for four experiments to control the SWI.

## 2.3 Numerical Modelling Approach

The SEAWAT program (Guo and Langevin 2002) was used to simulate SWI for the barrier wall and freshwater injection experiments. The SEAWAT program combines both MODFLOW and MT3DMS. In the variable-density flow (VDF) process of the SEAWAT program, the well-established MODFLOW is used as a familiar tool for solving the equations for the variable-density groundwater flow system by means of the finite-difference method (FDM) (Guo and Langevin 2002).

### 2.3.1 Subsurface Flow Barrier and Freshwater Injection Numerical Parameters

The dimension of the SEAWAT simulation were 75.0 cm × 35.0 cm in the horizontal and vertical directions respectively, as shown in Figure 2-A. The finite-difference grid interval was set at $\Delta x = \Delta y = 0.5$ cm. The freshwater head ($h_f$) and the saltwater head ($h_s$) were adjusted to 31.4 and 30.5 cm respectively. The saltwater concentration at the freshwater and saltwater boundaries was set to 0.0 and 35,000 mg/L respectively. The density of water in the freshwater and saltwater boundaries is set in the model to 1000 and 1025 kg/m$^3$ respectively. The initial concentration of the entire medium is 0.0 mg/L. The hydraulic conductivity and porosity values for the porous medium are similar to the experimental results of 0.60 cm/s and 0.43 respectively. Only the TVD (third- order total variation diminishing) scheme in the SEAWAT model code was used to solve the advection term. The values of numerical simulation parameters for flow and contaminant transport are shown in Table 2-A and Table 3-A for the barrier wall and freshwater injection experiments respectively. For freshwater injection
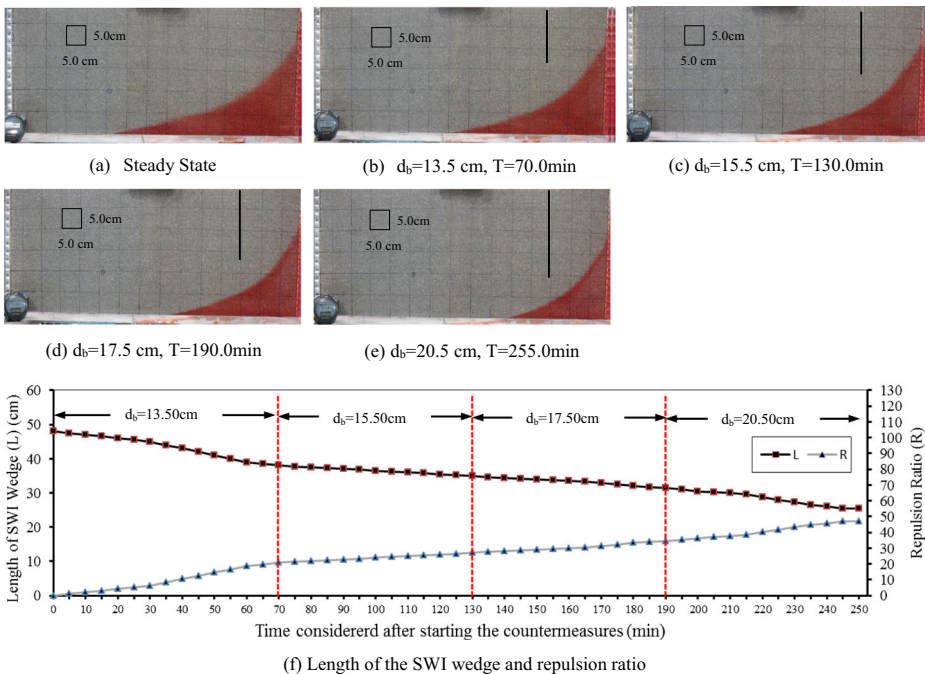


(a) Steady State  (b) $d_b$=13.5 cm, T=70.0min  (c) $d_b$=15.5 cm, T=130.0min

(d) $d_b$=17.5 cm, T=190.0min  (e) $d_b$=20.5 cm, T=255.0min

(f) Length of the SWI wedge and repulsion ratio

**Fig. 2** Experimental results of flow barrier wall **a** Steady state, **b** $d_b$ = 13.5 cm, **c** $d_b$ = 15.5 cm, **d** $d_b$ = 17.5 cm, **e** $d_b$ = 20.5 cm and **f** Length of the SWI wedge and repulsion ratio through the time

experiments, the freshwater injection points were set in the simulations at different locations outside the SWI wedge. The simulation of the effect of freshwater injection was repeated for different locations of the injection points located outside the SWI wedge, to determine the best location to achieve the maximum repulsion ratio of the saltwater wedge.

### 2.3.2 Sensitivity Analysis

A sensitivity analysis was performed to study the effect of barrier wall parameters, freshwater injection parameters and aquifer properties on the repulsion ratio R. Table 4-A summarizes the ranges of values of the parameters. In all the simulations, the initial condition corresponded to that of a steady-state saltwater wedge associated with a head difference of 9 mm, with a hydraulic gradient of 0.9/74.4.

The definitions of each of the parameters and the corresponding dimensionless ratios are:

| | |
|---|---|
| $d$ | is the unconfined coastal aquifer depth, |
| $d_b$ | is the barrier wall depth, |
| $X_b$ | is the distance from the barrier wall to the saltwater tank, |
| $L_o$ | is the initial length of the SWI wedge under steady-state conditions, |
| $L$ | is the length of the saltwater wedge, |
| $R$ | is the repulsion ratio of the SWI wedge $R = [(L_o-L)/L_o]$, |
| $X_i$ | is the distance from the injection point to the saltwater tank, |
| $Y_i$ | is the depth from the ground surface to the freshwater injection point, |
| $Q$ | is the flow rate under steady-state condition, |
| $Q_i$ | is the freshwater injection flow rate, |
| $d_b/d$ | is the barrier wall embedment ratio, |
| $X_b/L_o$ | is the ratio of horizontal distances from the saltwater tank to the barrier wall, |
| $X_i/L_o$ | is the ratio of horizontal distances from the saltwater tank to the freshwater injection point, |
| $Y_i/d$ | is the ratio of freshwater injection point depth to the aquifer depth and |
| $Q_i/Q$ | is the freshwater injection rate ratio. |

## 3 Results and Discussion

### 3.1 Experimental Results

#### 3.1.1 Effect of Barrier Wall on SWI Wedge (Experiment No. 1)

Figure 2 shows the steady-state results for the SWI wedge after installing the flow barriers at depths of $d_b$ = 13.5, 15.5, 17.5 and 20.5 cm. Figures 3-A and 4-A show images of the SWI wedge in experiment No. 1 at different time points. The average values of hydraulic conductivity and porosity are found to be 0.60 cm/s and 0.43 respectively. Figure 2a shows the initial steady-state condition for the SWI prior to flow barrier installation. The length of the SWI wedge in the steady-state condition is 48.00 cm, measured from the saltwater reservoir. After 70 min from the installation of the flow barrier to a depth of 13.5 cm, the SWI wedge had
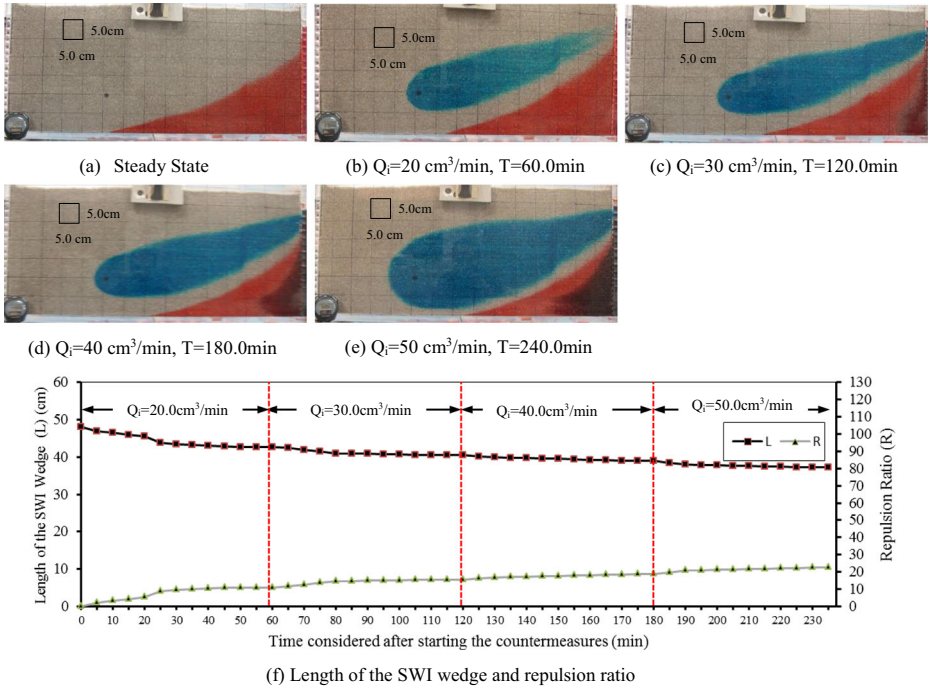
(a)  Steady State

(b) $Q_i=20$ cm³/min, T=60.0min

(c) $Q_i=30$ cm³/min, T=120.0min

(d) $Q_i=40$ cm³/min, T=180.0min

(e) $Q_i=50$ cm³/min, T=240.0min

(f) Length of the SWI wedge and repulsion ratio

**Fig. 3** SWI experiments results with injection rate **a** Steady state, **b** $Q_i = 20$ cm³/min, **c** $Q_i = 30$ cm³/min, **d** $Q_i = 40$ cm³/min, **e** $Q_i = 50$ cm³/min and **f** Length of the SWI wedge and repulsion ratio through the time



(a) $d_b=6.5$cm T=300.0min

(b) $d_b=9.5$cm, T=360.0min

(c) $d_b=11.5$cm, T=420.0min

(d) $d_b=13.5$cm, T=480.0min

(e) $d_b=15.5$cm, T=545.0min

(f) $d_b=17.5$cm, T=600.0min

(g) Length of the SWI wedge and repulsion ratio

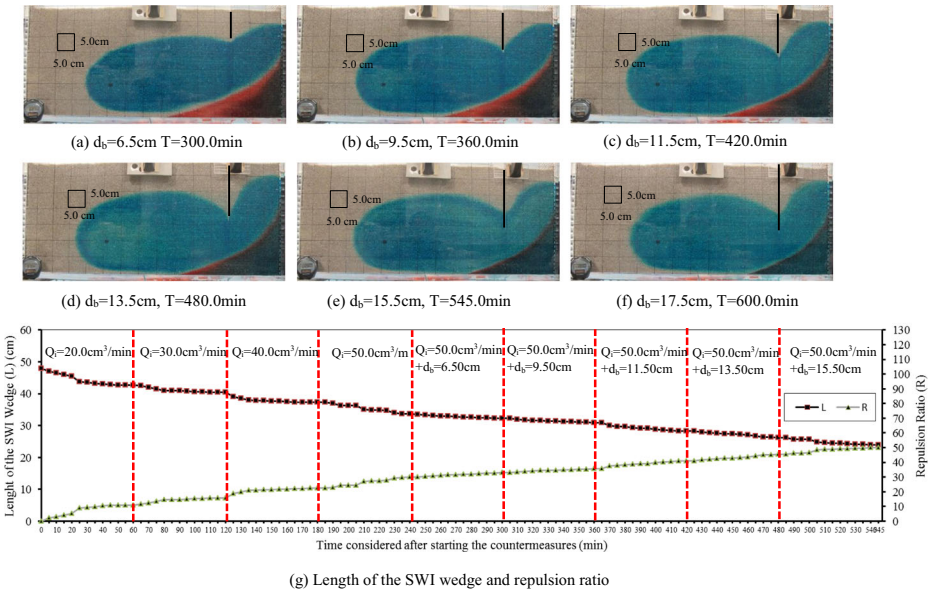**Fig. 4** SWI experiments results with combination of injection rate 50 cm³/min and barrier wall with depth **a** $d_b = 9.5$ cm, **b** $d_b = 9.5$ cm, **c** $d_b = 11.5$ cm, **d** $d_b = 13.5$ cm, **e** $d_b = 15.5$ cm, **f** $d_b = 17.5$ cm and **g** Length of the SWI wedge and repulsion ratio through the time

gradually retreated and the steady-state toe position had retreated to 38.0 cm, with a repulsion ratio of about 20.8% (Fig. 2b). Accordingly, the flow barrier depth was increased to 15.50, 17.50 and 20.5 cm, which led to the SWI wedge retreating more and the steady-state toe position retreating to 35.0, 31.5 and 25.5 cm, with repulsion ratios of about 27.8, 36.45 and 46.87% respectively (Fig. 2f). After the installation of the flow barrier in the aquifer medium, the freshwater-saltwater equilibrium is disturbed, and a new flow field is imposed. Decreasing the opening for the freshwater flow to the saltwater reservoir led to an increase in the flow velocity and also in the head of freshwater near to the flow barrier. The new pressure condition causes the SWI wedge to retreat. The deeper the flow barrier penetration, the smaller the opening from the freshwater to the saltwater reservoir and the greater the saltwater repulsion ratio achieved.

### 3.1.2 Effect of Freshwater Injection on SWI Wedge (Experiment No. 2)

Figure 3 shows the initial steady state of the SWI wedge and the resulting saltwater wedge after freshwater injection via point injection with rates $Q_i = 20, 30, 40$ and $50$ cm³/min. Figures 5-A and 6-A show images of the SWI wedge in experiment No. 2 at different time points. The initial steady-state length of the SWI wedge is 48.00 cm, measured from the saltwater reservoir side (Fig. 3a). After starting the freshwater injection at 20 cm³/min., the SWI wedge gradually retreats (Fig. 3b). Injecting the freshwater at rates of 20, 30, 40 and 50 cm³/min. Leads the SWI wedge to gradually retreat to 42.75, 40.50, 39.00 and 37.25 cm respectively, with values of R equals 10.93, 15.63, 18.75 and 22.39% respectively (Fig. 3f). The scenarios of the freshwater injection
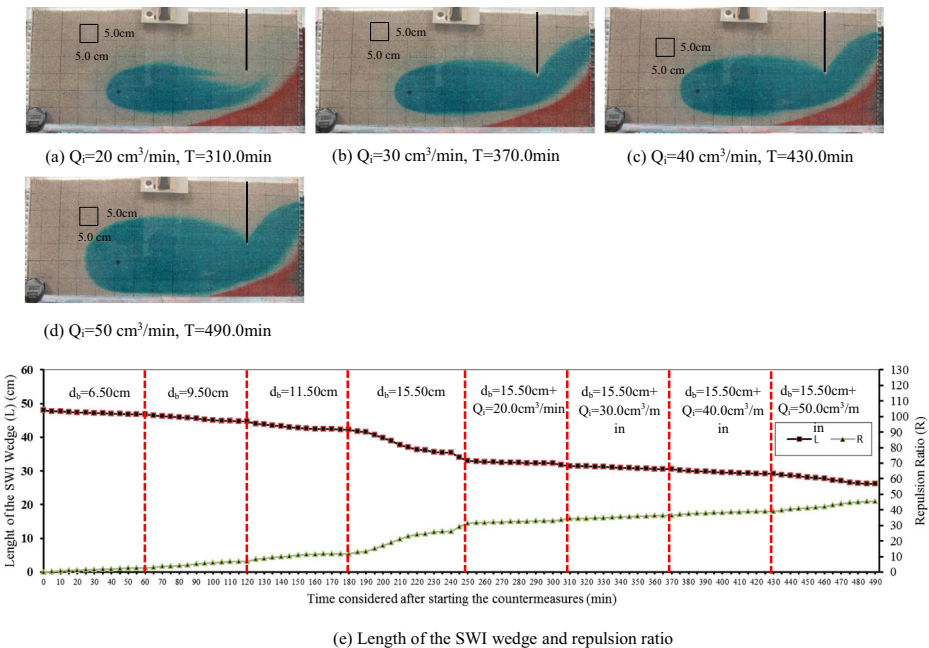


(a) $Q_i$=20 cm³/min, T=310.0min   (b) $Q_i$=30 cm³/min, T=370.0min   (c) $Q_i$=40 cm³/min, T=430.0min

(d) $Q_i$=50 cm³/min, T=490.0min

(e) Length of the SWI wedge and repulsion ratio

**Fig. 5** SWI experiments results with combination of barrier wall with depth $d_b = 15.5$ cm and injection rate **a** $Q_i = 20$ cm³/min, **b** $Q_i = 30$ cm³/min, **c** $Q_i = 40$ cm³/min, **d** $Q_i = 50$ cm³/min and **e** Length of the SWI wedge and repulsion ratio through the time
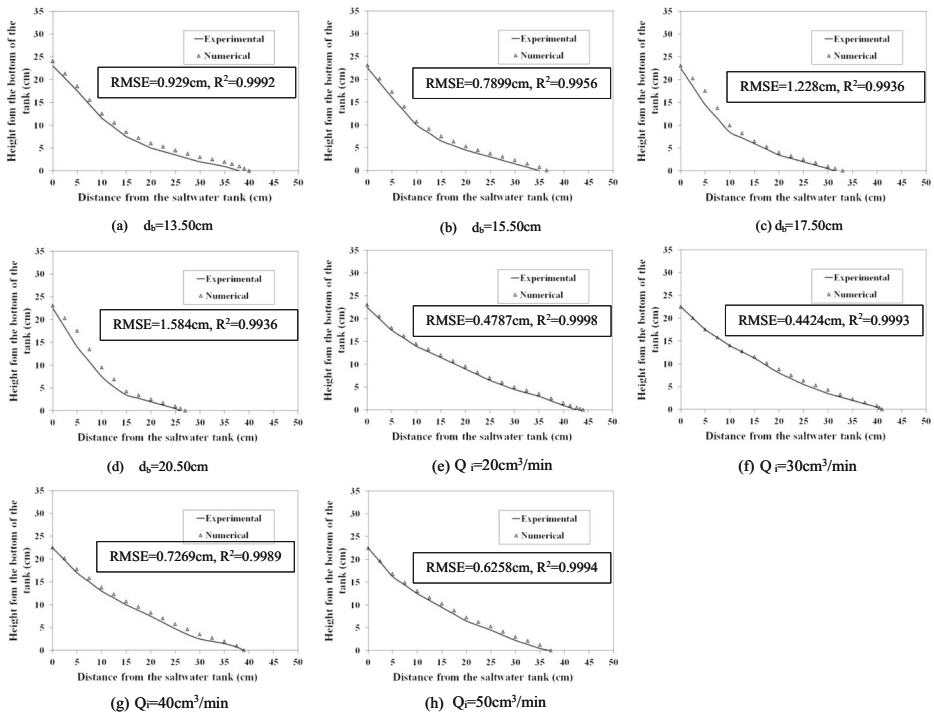
**Fig. 6** Comparison between SWI interface steady state experimental and numerical results of Experiment No.1 and No.2

experiments show that a more effective value of R is achieved with the highest values of injection flow rate. The most practicable freshwater injection rate should be applied, in order to achieve the maximum R of the SWI wedge.

### 3.1.3 Combined Effect of Barrier and Freshwater Injection on SWI Wedge

**The Effect of Variable Barrier Wall Depth with Constant Freshwater Injection (Experimental No. 3)** Figure 4 shows the SWI wedge for the combination of injection through a well with a constant rate of 50 cm³/min. and a barrier wall of depths $d_b = 6.5$, 9.50, 11.5, 13.5, 15.5 and 17.50 cm. Figures 7-A, 8-A and 9-A show images of the SWI wedge in experiment No. 3 at different time points. After 60.0 min. The toe position reaches the steady-state condition and the SWI wedge retreats to 33.60 cm with $R = 30.0\%$ for $d_b = 6.5$ cm (Fig. 4a). After a steady state is reached, the barrier wall is embedded further into the aquifer to a depth of 9.5, 11.5, 13.5, 15.5 and 17.5 cm, with a constant freshwater injection rate (50 cm³/min.) (Fig. 4b to f). Increasing the depth of the flow barrier to 9.50, 11.5, 13.5, 15.5 and 17.50 cm results in the SWI wedge retreating to 32.20, 30.90, 28.25, 26.2 and 24.00 cm, with R values of 32.90, 35.63, 41.15, 45.42 and 50.00% respectively (Fig. 4g). Increasing the depth of the barrier wall, with constant freshwater injection, has a significant impact on the SWI wedge. With increased flow barrier depth, the opening below the barrier wall decreases and the freshwater velocity to the saltwater side increases. As a consequence, the effect of the freshwater injection forces the SWI wedge to become more attenuated compared with the cases of freshwater injection or a barrier wall separately.
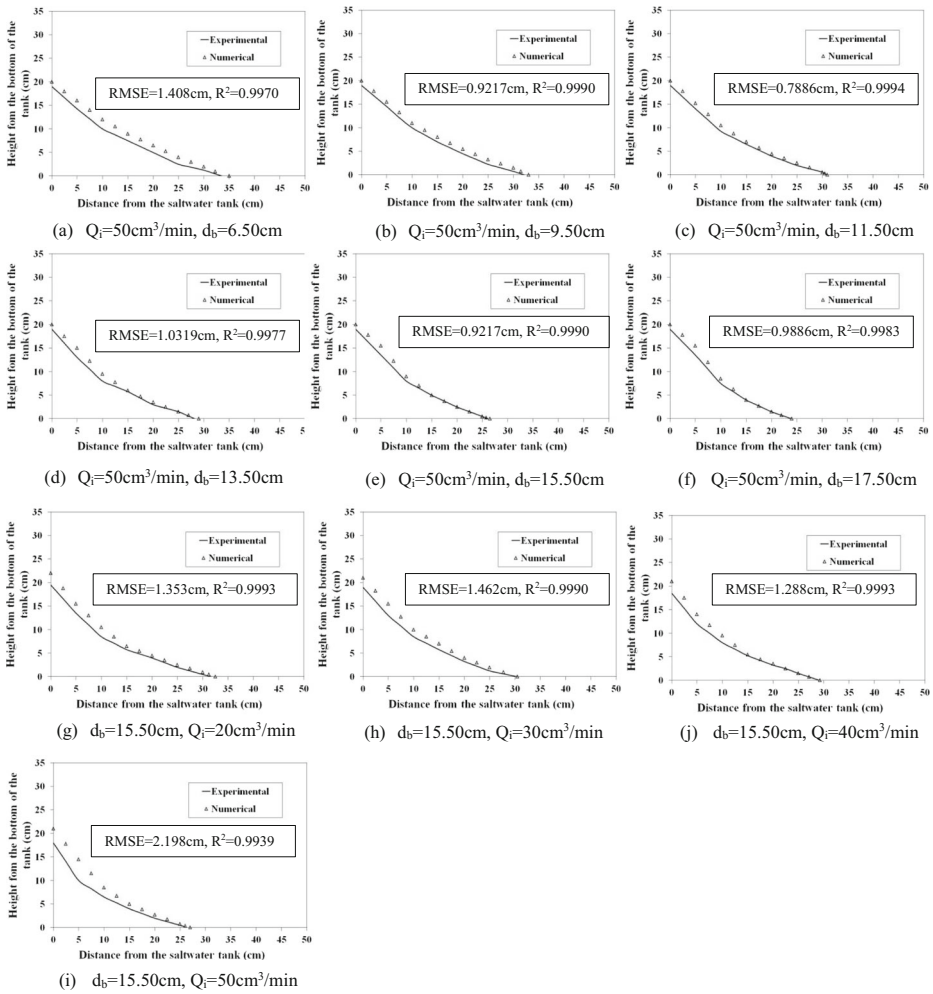
(a)  $Q_i=50cm^3/min$, $d_b=6.50cm$

(b)  $Q_i=50cm^3/min$, $d_b=9.50cm$

(c)  $Q_i=50cm^3/min$, $d_b=11.50cm$

(d)  $Q_i=50cm^3/min$, $d_b=13.50cm$

(e)  $Q_i=50cm^3/min$, $d_b=15.50cm$

(f)  $Q_i=50cm^3/min$, $d_b=17.50cm$

(g)  $d_b=15.50cm$, $Q_i=20cm^3/min$

(h)  $d_b=15.50cm$, $Q_i=30cm^3/min$

(j)  $d_b=15.50cm$, $Q_i=40cm^3/min$

(i)  $d_b=15.50cm$, $Q_i=50cm^3/min$

**Fig. 7** Comparison between SWI interface from steady state experimental and numerical results for Experiment No.3 and No.4

**The Effect of Variable Freshwater Injection with Constant Barrier Wall Depth (Experiment No. 4)** Figure 5 shows the SWI wedge for the combination of a barrier wall with constant depth of 15.5 cm and injection through a well at rates of 20.0, 30.0, 40.0 and 50.0 cm³/min. Figures 10-A and 11-A show images of the SWI wedge in experiment No. 4 at different time points. The injected flow and the flow from the freshwater to the saltwater passes through the opening below the barrier wall and force the SWI to become attenuated. The maximum repulsion ratio is observed after 60.0 min. For injection at 20.0 cm³/min., and the length of the SWI reduces to 31.75 cm with a repulsion ratio of 33.85% (Fig. 5a). When the freshwater injection rate was increased to 30.0, 40.0 and 50.0 cm³/min., the SWI lengths reduced to 30.50, 29.25 and 26.20 cm, with R values of 36.45, 39.06 and 42.45% respectively (Fig. 5b to f). Injection of freshwater through a well-combined with a constant barrier wall achieved higher values of R for the SWI wedge, compared with a flow barrier only. The injected flow and the flow from the

freshwater to the saltwater passes through the small opening below the barrier wall with high velocity and forces the SWI wedge to attenuate more at the saltwater side.

## 3.2 Verification Phase (Numerical Simulation)

### 3.2.1 Experiment No. 1 and No. 2

Figure 6a to d show the comparison between the experimental and numerical results for the SWI interface in cases with different barrier wall depths. The numerical SWI length in the steady state was 40.0, 36.5, 33.0 and 27.0 cm for flow barrier depths of 13.5, 15.5, 17.5 and 20.5 cm, compared with 38.0, 35.00, 31.5 and 25.5 cm respectively from experimental tests. Figure 6e to h show the comparison between the experimental and numerical results for the SWI interface for different freshwater injection rates. The numerical SWI length in the steady state was 44.00, 41.00, 39.00 and 37.50 cm for freshwater injection rates of 20, 30, 40 and 50 cm$^3$/min. Respectively, compared with 42.75, 40.50, 39.00 and 37.25 cm for the experimental tests. The results show good agreement in terms of the SWI wedge for steady-state condition.

### 3.2.2 Combination of Barrier Wall and Freshwater Injection [Experiment No. 3 and No. 4]

Figure 7a to f show the comparison between the steady-state experimental and numerical results for the SWI interface in the case of a combination of freshwater injection at a constant rate of 50.0 cm$^3$/min and a barrier wall with depths $d_b = 6.50$, 9.50, 11.50, 13.50, 15.50 and 17.50 cm. The length of the SWI wedge in the steady state was 35.0, 33.0, 31.0, 29.0, 26.5 and 24.0 cm, compared with 33.6, 32.2, 30.9, 28.25, 26.20 and 24.00 cm for the experimental results. Figure 7g to j show the comparison between the steady-state experimental and numerical results for the SWI interface in the case of a combination of a barrier wall with constant depth $d_b = 15.50$ cm and freshwater injection at flow rates of 20.0, 30.0, 40.0 and 50.0 cm$^3$/min. The length of the SWI wedge in the steady state was 32.25, 30.50, 29.25 and 27.0 cm, compared with 31.75, 30.5, 29.25 and 26.20 cm respectively for the experimental results. The comparison shows good agreement in terms of the SWI wedge under steady-state condition.

## 3.3 Results of Sensitivity Analysis

### 3.3.1 Impact of Barrier Wall Depth Ratio ($d_b$/d) on Repulsion Ratio (R)

The sensitivity of the repulsion ratio (R) with respect to the barrier wall depth was explored for seven different barrier wall depth ratios ($d_b$/d) (Table 4-A) (Fig. 8a) with fixed $Q_i$/Q = 50/90, for two different injection well depth ratios ($Y_i$/d = 20/48 and 25/48) and for two well location ratios ($X_i$/$L_o$ = 1.0 and 1.20). Increasing the embedment depth of the flow barrier combined with freshwater injection through the well led to the SWI retreating further and increased the repulsion ratio R. The ratio R increased from 25.0 to 52.0% when $d_b$/d increased from 21.0 to 67.0%, in the case of injection of freshwater through a point above the toe point at $X_i = 1.00L_o$ and $Y_i$/d = 20/30.5. R was increased further from 52 to 62% by increasing $Y_i$/d to 25/30.5 (Fig. 8a).
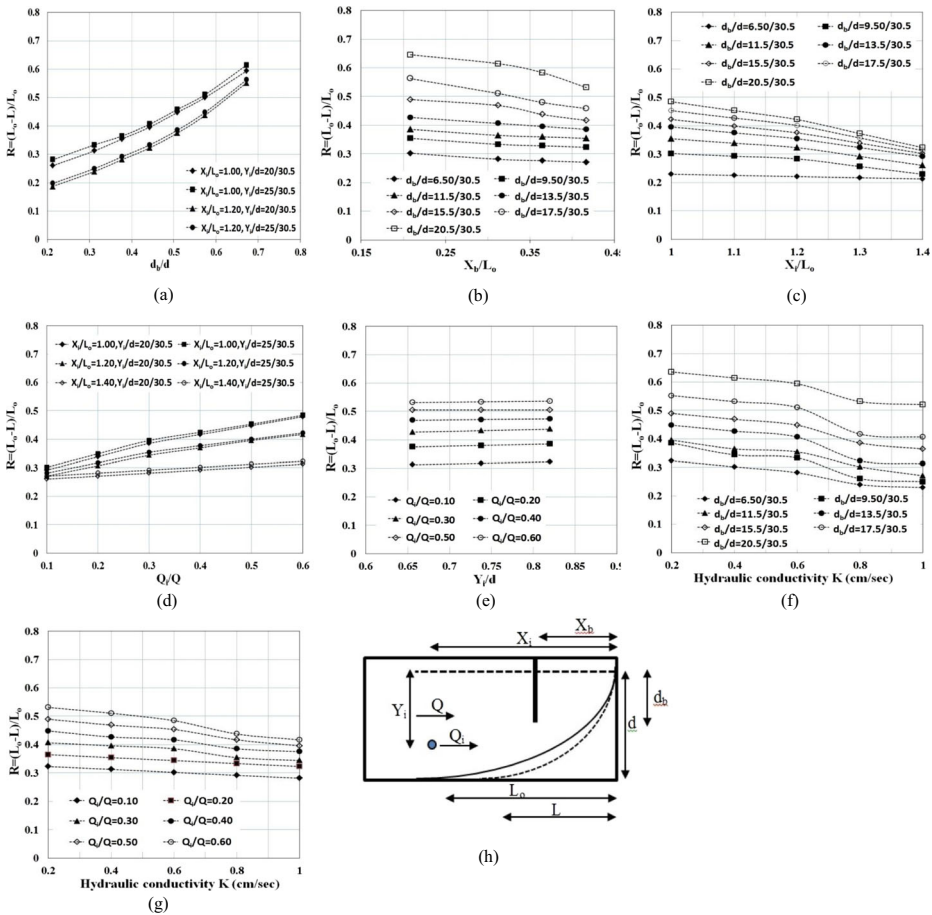
**Fig. 8** Sensitivity analysis of repulsion ratio R to **a** $d_b/d$, **b** $X_b/L_o$, **c** $Q_i/Q$, **d** $X_i/L_o$, **e** $Y_i/d$, **f** K with $d_b/d$ and **g** K with $Q_i/Q$, **h** Legend

### 3.3.2 Impact of Barrier Wall Location Ratio ($X_b/L_o$) on Repulsion Ratio (R)

The sensitivity of R to the barrier wall distance ratio $X_b/L_o$ was tested for four different distance ratios (10/48, 15/48, 17.5/48 and 20/48), for seven different barrier depth ratios ($d_b/d$) (Fig. 8b). R increases with the movement of the flow barrier towards the saltwater side. The maximum value of the repulsion ratio (64%) is achieved when $X_b/d = 10/48$ and $Y_i/d = 20/30.5$ (Fig. 8b). Moving the point of freshwater injection to $X_i = 1.2L_o$ gives a lower repulsion ratio than for $X_i = 1.0L_o$.

### 3.3.3 Impact of Freshwater Injection Rate Ratio ($Q_i/Q$) on Repulsion Ratio (R)

In this section, the impact of injection rate ratio ($Q_i/Q$) on R was assessed for six different injection ratios ($Q_i/Q$) (Fig. 8c). This was done for six different well locations $X_i/L_o$ and $Y_i/d$, with a fixed barrier wall depth ratio $d_b/d = 15.5/30.5$. An increase in $Q_i/Q$ combined with a constant barrier wall depth leads to the SWI retreating further. R increased from 30 to 48.44% when $Q_i/Q$ increased from 0.1 to 0.6.

### 3.3.4 Impact of Freshwater Injection Distance Ratio ($X_i/L_o$) on Repulsion Ratio (R)

The sensitivity of R to freshwater injection depth ($Y_i/d$) was tested for three different depths (20/30.5, 22.5/30.5 and 25/30). This was performed with constant $d_b/d = 20/30.5$ and $X_b/L_o = 15/48$ for six different injection rate ratios (Fig. 8d). R increased from 53 to 54% as $Y_i/d$ increased from 20/30.5 to 25/30.5.

### 3.3.5 Impact of Freshwater Point Depth Ratio ($Y_i/d$) on Repulsion Ratio (R)

The effect of injection point distance $X_i/L_o$ on R was assessed for four different distances $X_i/L_o = 1.0$, 1.2, 1.3 and 1.4, with a constant $Q_i/Q = 50/90$ and for seven barrier depth ratios $d_b/d$ (Fig. 8e). Moving the point of freshwater injection to $X_i = 1.4L_o$ gives lower repulsion ratios compared with $X_i = 1.0L_o$. The repulsion ratio decreased from 48.4 to 38.2% when $X_i/L_o$ increased from 1.0 to 1.4.

### 3.3.6 Impact of Hydraulic Conductivity (K) on Repulsion Ratio (R)

To study the impact of hydraulic conductivity on R, five different values of K were considered: 0.2, 0.4, 0.6, 0.8 and 1.0 cm/s, for two cases. The first case was with constant $Q_i/Q = 50/90$, $X_i/L_o = 1.0$ and $Y_i/d = 20/30.5$ for seven different $d_b/d$ values (Fig. 8f). The second case was with fixed $d_b/d = 20/30.5$ and $X_b/L_o = 15/48$ for six different $Q_i/Q$ values. An increase in K led to an increase in the SWI length (Fig. 8g). Increasing K from 0.2 to 1.0 cm/s led to a decrease in R from 63 to 52% with $d_b/d = 25/30$. The maximum R was observed for higher $Q_i/Q$ values, but R decreased from 53 to 42% as K increased from 0.2 to 1.0 cm/s.

### 3.3.7 Impact of Hydraulic Gradient ($i$) on Repulsion Ratio (R)

The sensitivity of R to the hydraulic gradient was assessed for five different values and two cases. Firstly, with constant $Q_i/Q$ (50/90), $X_i/L_o$ (1.0), $Y_i/L_o$ (25/48) and $X_b/L_o$ (15/48), for different $d_b/d$ values (Fig. 9a). Secondly, was with constant $d_b/d$ (20/30.5), $X_b/L_o$ (15/48) and $X_i/L_o$ (1.0) for six different values of $Q_i/Q$ (Fig. 9b). Increasing $i$ led to the SWI retreating further. Increasing $i$ from 0.7/74.4 to 1.1/74.4 led to an increase in R from 20.8 to 71.8% with an embedment barrier wall with ratio $d_b/d = 20/30.5$ and constant $Q_i/Q = 50/90$. For constant $d_b/d = 20/30.5$, increasing $Q_i/Q$ from 0.1 to 0.6 increased R from 26 to 64.5%.

### 3.3.8 Impact of Porosity ($n$) on Repulsion Ratio (R)

In this section, the impact of porosity $n$ on the repulsion ratio R was tested for four different porosity values of 0.15, 0.25, 0.35 and 0.4, for two cases. The first case was for seven different $d_b/d$ values, with fixed $Q_i/Q = 50/90$, $X_i/L_o = 1.0$, $Y_i/L_o = 25/48$ and $X_b/L_o = 15/48$ (Fig. 9c). The second case was for six different injection rate ratios $Q_i/Q$ with fixed values of $d_b/d$ (20/30), $X_b/L_o$ (15/48) and $X_i/L_o$ (1.0) (Fig. 9d). Increasing $n$ from 0.15 to 0.4 led to the SWI intruding further and R decreasing from 62 to 59%, with $d_b/d$ increasing to 20/30.5 and constant $Q_i/Q$.

### 3.3.9 Impact of Saltwater Density ($\rho_s$) on Repulsion Ratio (R)

To study the effect of saltwater density on R, five different values of $\rho_s$ were used in two separate simulations: 1018, 1022, 1025, 1027 and 1030 kg/m$^3$, with corresponding saltwater concentrations
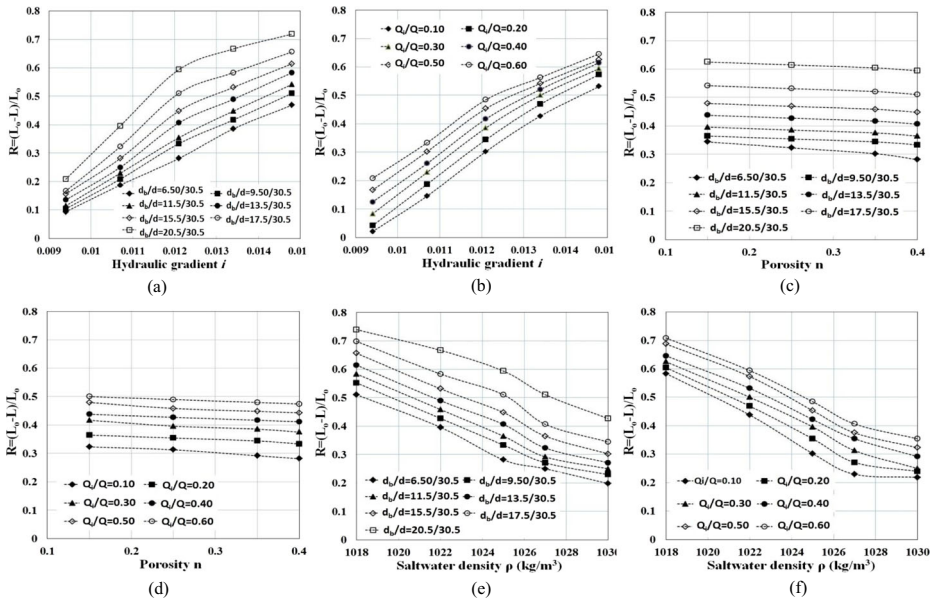
**Fig. 9** Sensitivity analysis of repulsion ratio R to **a** $i$ with $d_b/d$, **b** $i$ with $Q_i/Q$, **c** $n$ with $d_b/d$, **d** $n$ with $Q_i/Q$, **e** $\rho_s$ with $d_b/d$ and **f** $\rho_s$ with $Q_i/Q$

of 25,000, 30,000, 35,000, 37,500 and 40,000 mg/L respectively. The first case was tested with fixed $Q_i/Q$ (50/90), $X_i/L_o$ (1.0) and $Y_i/d$ (15/30.5), for seven different $d_b/d$ values (Fig. 9e). The second case was with fixed $d_b/d$ (15/30.5) and $X_b/L_o$ (15/48) for six different $Q_i/Q$ values (Fig. 9f). Increasing $\rho_s$ from 1018 to 1030 kg/m³, led to the SWI intruding further into the aquifer and a decrease in R from 73 to 42%, with constant $Q_i/Q = 50/90$ and $d_b/d$ reaching 20/30.5. In addition, R decreased by half from 70.8% to around 35% when $\rho_s$ increased from 1018 to 1030 kg/m³ with constant $d_b/d = 20/30.5$ and $Q_i/Q$ increased to 50/90.

# 4 Conclusion

Decreasing the opening for the flow from the freshwater reservoir to the saltwater reservoir led to an increase in the flow velocity below the flow barrier and also in the head of freshwater near to the flow barrier. The new pressure condition forced the SWI wedge to retreat. The deeper the flow barrier penetration, the smaller of the opening from the freshwater to the saltwater reservoir and the greater the saltwater repulsion ratio achieved. Increasing the barrier wall embedment ratio ($d_b/d$) from 0.44 to 0.67 led to R increasing from 20.8 to 46.87%.

On the other hand, the scenarios of the freshwater injection experiments through an injection point confirmed that the most effective value of repulsion ratio of the SWI wedge was achieved with the highest value of injection flow rate. The most practicable freshwater injection rate should be applied in order to achieve maximum R. Increasing the freshwater injection ratio ($Q_i/Q$) through point injection from 0.22 to 0.56 led to the repulsion ratio increasing from 10.93 to 22.39%.

Embedding the barrier wall into the aquifer after injecting the freshwater through the well, as a combined method of controlling the SWI in unconfined coastal aquifers achieved greater

R for the SWI compared with a barrier wall or freshwater injection separately. Embedding the barrier wall further into the aquifer leads to a decrease in the opening below the barrier wall and an increase in the pressure head and the flow from the freshwater to the saltwater side, which forces the SWI to become attenuated towards the saltwater side. Embedding the barrier wall with ratios $d_b/d$ of 0.44, 0.51 and 0.57 combined with constant freshwater injection with a $Q_i/Q$ ratio of 0.556 gave R values of 41.14, 45.41 and 50.0% respectively, compared with 20.8, 27.1 and 34.40% for the barrier wall only and 22.39% for freshwater injection only. Based on the numerical analysis, embedding the barrier close to the saltwater side combined with freshwater injection achieved a maximum R of about 68.0%.

Injection of the freshwater through the well after embedding the barrier wall, as a combined method of controlling the SWI in unconfined coastal aquifers, achieved greater R values for the SWI compared with the barrier wall or freshwater injection separately. The injected flow and the flow from the freshwater to the saltwater passed through the remaining opening below the barrier wall and forced the SWI become attenuated towards the saltwater side. Injecting freshwater with $Q_i/Q$ ratios of 0.22, 0.33, 0.44 and 0.56, combined with a constant embedment barrier wall with ratio $d_b/d = 0.508$ led to R values of 33.9, 36.5, 39.0 and 45.42%, compared with 10.9, 15.6, 18.8 and 22.4% respectively for freshwater injection only and 27.1% for the barrier wall only. Based on the numerical analysis, increasing the injection rate of freshwater combined with placing the barrier wall close to the saltwater side achieved a repulsion ratio of about 52.0%. It can be concluded that the combination of flow barrier wall and freshwater injection through the well forces the saltwater to attenuate and achieves a greater repulsion ratio R compared with using the flow barrier wall or the freshwater injection technique separately.

## Compliance with Ethical Standards

**Conflict of Interest**   None.

**Publisher's Note** Springer Nature remains neutral with regard to jurisdictional claims in published maps and institutional affiliations.

## References

Abdoulhalik A, Ahmed AA (2017) The effectiveness of cutoff walls to control saltwater intrusion in multi-layered coastal aquifers: experimental and numerical study. J Environ Manag 199:62e73
Abdoulhalik A, Ashraf A, Hamill G (2017) A new physical barrier system for seawater intrusion control. J Hydrol 549:416e427
Anwar H (1983) The effect of a subsurface barrier on the conservation of freshwater in coastal aquifers. Water Res 17:1257e1265
Attanayake P, Sholley M (2007) Evaluation of the hydraulic gradient at an island for low-level nuclear waste disposal. IAHS Publ 312:237–243
Bear J (1979) Hydraulics of groundwater. McGraw- Hill Book Co., Inc., New York
Bruington AE, Seares FD (1965) Operating a seawater barrier project. J Irrig Drain Eng 91(1):117–140
Chang SW, Clement TP (2012) Experimental and numerical investigation of saltwater intrusion dynamics in flux-controlled groundwater systems. Water Resour Res 48:W09527

Goswami RR, Clement TP (2007) Laboratory-scale investigation of saltwater intrusion dynamics. Water Resour Res 43:W04418

Guo W, Langevin CD (2002) User's guide to SEAWAT: a computer program for simulation of three-dimensional variable-density ground-water flow. U.S. Geol. Surv., Reston

Hasan Basri M (2001) Two new methods for optimal design of subsurface barrier to control seawater intrusion. PhD Thesis. The Univ. of Manitoba

Hunt B (1985) Some analytical solutions for seawater intrusion control with recharge wells. J Hydrol 80(1–2):9–18

IPCC (2013) Summary for policymakers. In: Climate change 2013: the physical science basis. Contribution of working group I to the fifth assessment report of the intergovernmental panel on climate change. Ipcc

Luo P, Zhou M, Deng H, Lyu J, Cao W, Takara K, Nover D, Schladow SG (2018a) Impact of forest maintenance on water shortages: hydrologic modeling and effects of climate change. Sci Total Environ 615:1355–1363

Luo P, APIP, He B, Duan W, Takara K, Nover D (2018b) Impact assessment of rainfall scenarios and land-use change on hydrologic response using synthetic area IDF curves. Journal of Flood Risk Management 11:S84–S97. https://doi.org/10.1111/jfr3.12164

Luyun RA (2010) Effects of subsurface physical barrier and artificial recharge on seawater intrusion in coastal aquifers. PhD thesis. Kagoshima University, Japan

Luyun R Jr, Momii K, Nakagawa K (2009) Laboratory-scale saltwater behavior due to subsurface cutoff wall. J Hydrol 377:227e236

Luyun R Jr, Momii K, Nakagawa K (2011) Effects of recharge wells and flow barriers on seawater intrusion. Ground Water 49(2):239–249

Strack ODL (1976) A single-potential solution for regional interface problems in coastal aquifers. Water Resour Res 12(6):1165–1174

USEPA (2017) Report to congress: class V UIC study fact sheet - aquifer recharge Wells and aquifer storage and recovery Wells, EPA/ 816-R-99-014t. Office of Groundwater and Drinking Water, Washington, DC

## Affiliations

Asaad M. Armanuos[1] · Mona G. Ibrahim[2] · Wael Elham Mahmod[2,3] · Jiro Takemura[4] · C. Yoshimura[5]

Mona G. Ibrahim
mona.gamal@ejust.edu.eg

Wael Elham Mahmod
wael.elham@ejust.edu.eg; wdpp2006@aun.edu.eg

Jiro Takemura
takemura.j.aa@m.titech.ac.jp

C. Yoshimura
yoshimura.c.aa@m.titech.ac.jp

[1]    Department of Irrigation and Hydraulics Engineering, Faculty of Engineering, Tanta University, Tanta, Egypt

[2]    Egypt-Japan University of Science and Technology, Alexandria, Egypt

[3]    Civil Engineering Department, Faculty of Engineering, Assiut University, Asyut, Egypt

[4]    Department of Civil Engineering, Tokyo Institute of Technology, 2-12-1 Oookayama, Meguro, Tokyo 152-8552, Japan

[5]    Department of Civil Engineering, Tokyo Institute of Technology, 2-12-1 Oookayama, Meguro, Tokyo 152-0033, Japan